

# Supporting Information

## Flexible Three-Dimensional Net for Intravascular Fishing of Circulating Tumor Cells

*Shi-Bo Cheng,<sup>†</sup> Ming Wang,<sup>‡</sup> Chi Zhang,<sup>#</sup> Miao-Miao Chen,<sup>†</sup> Yi-Ke Wang,<sup>†</sup> Shan Tian,<sup>‡</sup> Na Zhan,<sup>‡</sup> Wei-Guo Dong,<sup>‡</sup> Min Xie,<sup>†\*</sup> Wei-Hua Huang<sup>†\*</sup>*

<sup>†</sup> College of Chemistry and Molecular Sciences, Wuhan University, Wuhan 430072, China

<sup>#</sup> Key Laboratory of Biomedical Polymers of Ministry of Education, College of Chemistry and Molecular Sciences, Wuhan University, Wuhan 430072, P. R. China

<sup>‡</sup> Renmin Hospital of Wuhan University, Wuhan 430060, China

\* E-mail: [whhuang@whu.edu.cn](mailto:whhuang@whu.edu.cn), [mxie@whu.edu.cn](mailto:mxie@whu.edu.cn)

The Supporting Information is available free of charge on the ACS Publications website: Figures S1-S1 and Table S1.

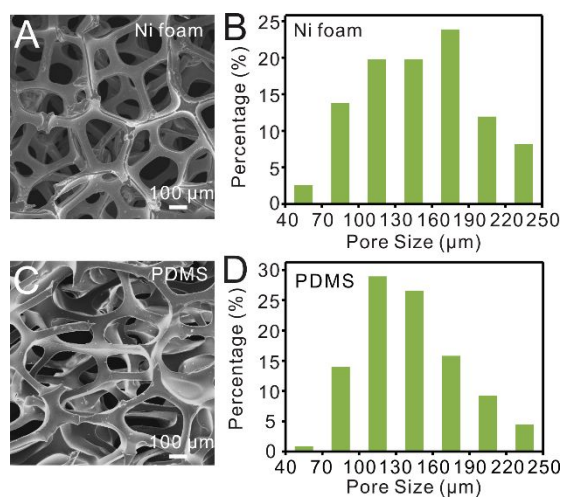


Figure. S1 SEM images and pore size distribution of Ni foam (A, B) and PDMS scaffold (C, D), respectively.

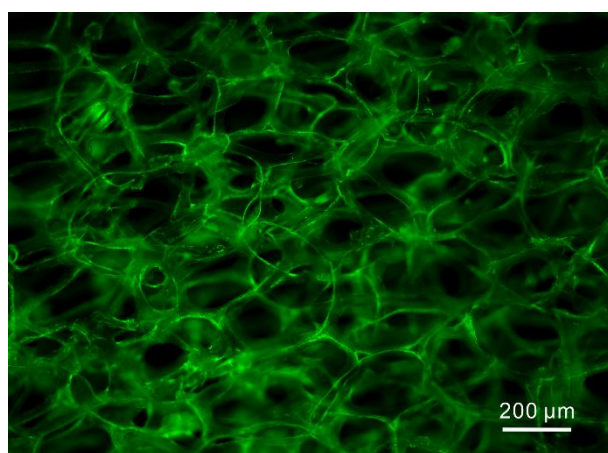


Figure. S2 Fluorescent image of anti-EpCAM antibody functionalized 3-D PDMS scaffold labelled by DyLight 488 conjugated goat anti-mouse IgG.

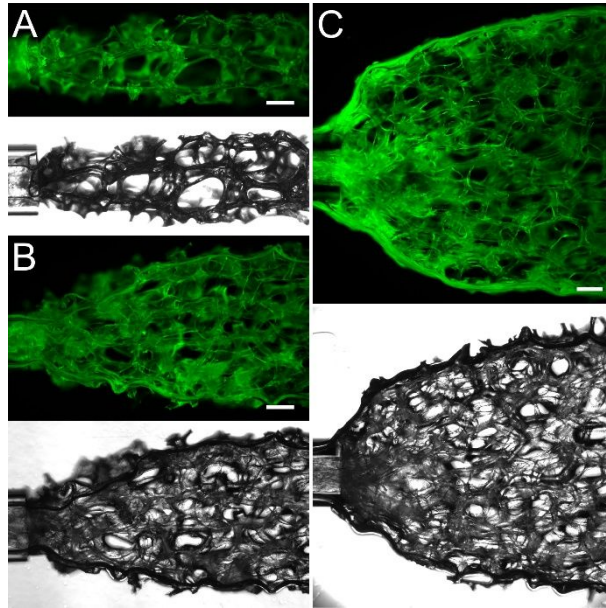


Figure. S3 Fluorescent and bright field images of CTC-Net probes with different size of 3-D PDMS scaffold tips. (A) width 0.8 mm, (B) width 1.6 mm, (C) width 3.2 mm. The anti-EpCAM antibody-functionalized 3-D scaffold was labelled by DyLight 488 conjugated goat anti-mouse IgG. Scale bar = 200  $\mu$ m



Figure. S4 Process of CTC-Net probe inserted into blood vessel.

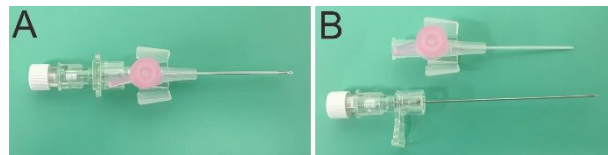


Figure. S5 Composition of indwelling needle. (A) A complete indwelling needle; (B) the steel needle and flexible pipe.

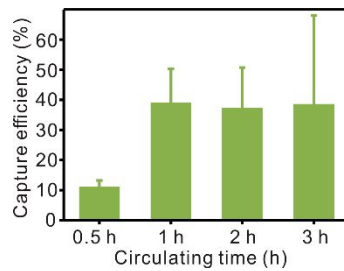


Figure. S6 Effect of indwelling time on capture efficiency (200 cells spiked in PBS for circulation) at the flow rate of 5 cm/s.

The indwelling time of CTC-Net in blood vessel influenced in capture efficiency which was evaluated by the simulated blood circulation system. Two hundred of DiI-stained MCF-7 cells spiked in PBS were circulated under the flow velocity of 5 cm/s, and CTC-Net was inserted and indwelled for different time (0.5, 1, 2 and 3 h). After that, the CTC-Net probe was taken out to count cancer cells under fluorescence microscope. As shown in Figure. S6, the long indwelling time tends to induce high capture efficiency, and capture efficiency increased from  $11 \pm 2\%$  to  $39 \pm 11\%$  along with 0.5 h and 1 h circulation, but it was not improved much after extending indwelling time to 2 h or 3 h. In order to get equilibrium between capture efficiency and detection time, 1 h was selected as the optimum indwelling time in the following experiments.

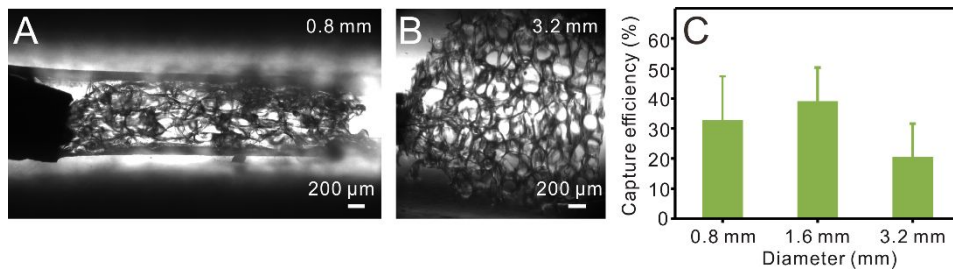


Figure. S7 CTC-Net probe with 3-D PDMS scaffold tip inserted into the rubber tube under fluid flow for mimicking the state of CTC-Net inside the blood vessel. (A, B) The inside diameter of rubber tube is 0.8 (A) and 3.2 mm (B), respectively; (C) Capture efficiencies in three kinds of rubber tubes with inside diameter of 0.8, 1.6, 3.2 mm, respectively at the flow rate of 5 cm/s.

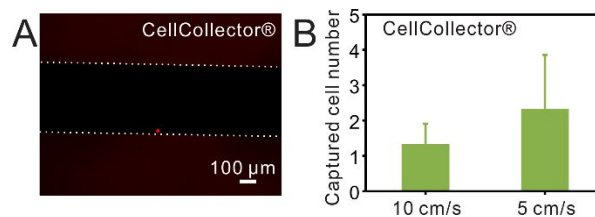


Figure. S8 *In vivo* capture of tumor cells from the simulated blood circulation system. (A) Fluorescent image of tumor cells captured on the GILUPI CellCollector®; (B) Quantitative results of GILUPI CellCollector® capturing of tumor cells.



Figure. S9 The nude rats with exogenous tumor.

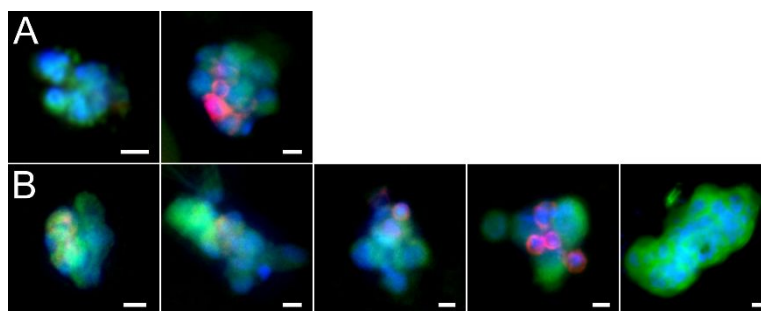


Figure. S10 *In vivo* captured CTC clusters by CTC-Net probe from tumor bearing nude rats of 2# (A) and 3# (B). All scale bar = 10  $\mu\text{m}$ .

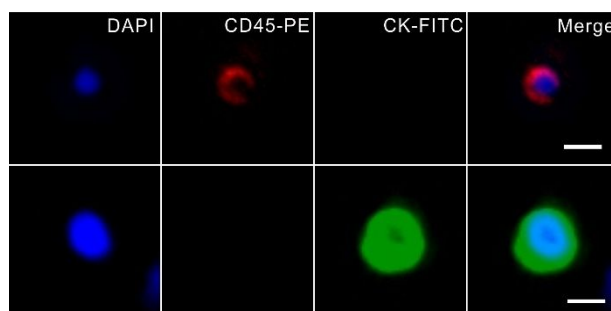


Figure. S11 Representative CTC captured by 3-D scaffold chip from 40  $\mu\text{L}$  of blood of tumor bearing nude rat. All scale bar = 10  $\mu\text{m}$ .

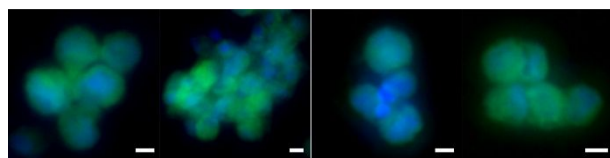


Figure. S12 CTC clusters captured by 3-D scaffold chip from 40  $\mu\text{L}$  of blood of 3# tumor bearing nude rat. All scale bar = 10  $\mu\text{m}$ .

Table S1 *In vivo* and *in vitro* capture of cancer cells from wild type rats.

Injected cell number	<i>In vivo</i> capture number	<i>In vivo</i> capture efficiency (%)	<i>In vitro</i> capture number	<i>In vitro</i> capture efficiency (%)
288 $\pm$ 14	26 $\pm$ 11	9.03 $\pm$ 3.94	0	0
1366 $\pm$ 286	53 $\pm$ 7	3.95 $\pm$ 0.33	0	0
6670 $\pm$ 523	66 $\pm$ 11	0.99 $\pm$ 0.13	3 $\pm$ 2	0.045 $\pm$ 0.029
28850 $\pm$ 1550	91 $\pm$ 12	0.31 $\pm$ 0.026	10 $\pm$ 4	0.036 $\pm$ 0.016

